Available online at www.sciencedirect.com
ScienceDirect
Applied Geochemistry 22 (2007) 2664–2683
Applied Geochemistry
www.elsevier.com/locate/apgeochem

Centimeter-scale characterization of biogeochemical gradients at a wetland–aquifer interface using capillary electrophoresis

Susan Báez-Cazull [a], Jennifer T. McGuire [a,*], Isabelle M. Cozzarelli [b], Anne Raymond [a], Lisa Welsh [a]

[a] *Texas A&M University, 3115 TAMU College Station, TX 77843, United States*
[b] *US Geological Survey, 431 National Center, Reston, VA 20192, United States*

Available online 21 June 2007

Abstract

Steep biogeochemical gradients were measured at mixing interfaces in a wetland–aquifer system impacted by landfill leachate in Norman, Oklahoma. The system lies within a reworked alluvial plain and is characterized by layered low hydraulic conductivity wetland sediments interbedded with sandy aquifer material. Using cm-scale passive diffusion samplers, "peepers", water samples were collected in a depth profile to span interfaces between surface water and a sequence of deeper sedimentary layers. Geochemical indicators including electron acceptors, low-molecular-weight organic acids, base cations, and NH_4^+ were analyzed by capillary electrophoresis (CE) and field techniques to maximize the small sample volumes available from the centimeter-scale peepers. Steep concentration gradients of biogeochemical indicators were observed at various interfaces including those created at sedimentary boundaries and boundaries created by heterogeneities in organic C and available electron acceptors. At the sediment–water interface, chemical profiles with depth suggest that SO_4^{2-} and Fe reduction dominate driven by inputs of organic C from the wetland and availability of electron acceptors. Deeper in the sediments (not associated with a lithologic boundary), a steep gradient of organic acids (acetate maximum 8.8 mM) and NH_4^+ (maximum 36 mM) is observed due to a localized source of organic matter coupled with the lack of electron acceptor inputs. These findings highlight the importance of quantifying the redox reactions occurring in small interface zones and assessing their role on biogeochemical cycling at the system scale.

1. Introduction

To understand and predict the fate and transport of numerous chemical species, including nutrients and contaminants, it is important to identify the most active zones of biogeochemical cycling within a system. It has been proposed that in natural systems, zones with steep biogeochemical gradients may be areas of increased microbial activity (Kappler et al., 2005). Microbial activity is enhanced when concentration gradients of limiting electron acceptors and/or electron donors come in contact, such as in the transition zones between environments of differing redox potential (Koretsky et al., 2003; Llobet-Brossa et al., 2002; McMahon and Chapelle, 1991; Sass et al., 2002; Ulrich et al., 1998). Although the potential importance of transition zones is widely accepted, characterization is challenging because chemical and microbiological

* Corresponding author.
E-mail address: mcguire@geo.tamu.edu (J.T. McGuire).

0883-2927/$ - see front matter © 2007 Elsevier Ltd. All rights reserved.
doi:10.1016/j.apgeochem.2007.06.003

measurements must be collected at sufficiently fine spatial resolution to describe resulting gradients. The microbial processes that control natural attenuation of contaminants typically occur at the μm to mm scale, yet measurements of electron acceptor and donor concentrations are most often made at the meter scale (Kappler et al., 2005). Here, findings of steep biogeochemical gradients observed at cm-scale transition zones in an aquifer–wetland system impacted by landfill leachate are presented.

The reduction–oxidation (redox) potential of a system, influenced by linked hydrological, microbiological and geochemical processes, largely controls the elemental cycling of nutrients and contaminants (Lyngkilde and Christensen, 1992; Nicholson et al., 1983; Peterson and Sun, 2000). In subsurface systems, much work has focused on documenting redox zonation and associated biodegradation at the plume scale. Many studies have suggested a sequential pattern of redox zones, each of which is dominated by a single terminal electron accepting process (TEAP) coupled to the oxidation of organic compounds (Baun et al., 2003; Chapelle and Mcmahon, 1991; Christensen et al., 2000; McGuire et al., 2000). Based on thermodynamic energy yield, microorganisms first use O_2 as an electron acceptor followed by the reduction of alternate electron acceptors including NO_3^-, Fe(III), SO_4^{2-}, and CO_2 (methanogenesis). This results in the characteristic redox zonation observed in sediments (Achtnich et al., 1995; Albrechtsen and Christensen, 1994; Champ et al., 1979; Chapelle et al., 1996; Christensen et al., 2000; Cozzarelli et al., 2000; Lovley and Phillips, 1987; Ludvigsen et al., 1998). However, studies have found TEAPs appear to occur simultaneously at the plume scale, thereby adding complexity to this sequential redox zone model (Blodau et al., 1998; Koretsky et al., 2003; Ludvigsen et al., 1998; McGuire et al., 2002; Motelica-Heino et al., 2003). Complexities in the distribution of TEAPs have also been identified at the "fringe" zones surrounding contaminant plumes where anoxic water contacts more oxic recharge water, creating gradients of electron acceptors and donors (Christensen et al., 2000; Mayer et al., 2001; Tuxen et al., 2006; van Breukelen and Griffioen, 2004; van Breukelen et al., 2003). Similarly, heterogeneities in the spatial distribution of sediments (e.g., particle size, mineralogy), organic C content, and availability of electron acceptors can allow for the coexistence of several C oxidation pathways using multiple electron acceptors (Koretsky et al., 2003). Complexities in the redox zonation model illustrate the importance of collecting biogeochemical measurements at sufficiently small spatial intervals to characterize the active zones of biogeochemical cycling. For example, studies by Cozzarelli et al. (2001) and Bekins et al. (2001) observed that Fe reduction gradients occurred at centimeter scales in a hydrocarbon contaminated plume due to the heterogeneous distribution of reducible Fe minerals.

Quantifying the redox reactions occurring at these relatively small transition zones may be critical to assessing the overall biogeochemical cycling in a system if these zones are indeed areas of enhanced microbial activity. Previous studies have documented enhanced microbial activity at interface zones created by lithologic boundaries (Ulrich et al., 1998) and surface water–groundwater interfaces (Dahm et al., 1998) due to the mixing of electron donors and acceptors. Steep geochemical gradients of metabolic byproducts (i.e. organic acids) have also been observed at the interface between aquifer and aquitard sediments (McMahon and Chapelle, 1991). In a recent study, Tuxen et al. (2006) documented a steep gradient of phenoxy acids and O_2 at the fringe of a contaminant plume where microbial degradation was enhanced, demonstrating the importance of measuring these gradients at small (decimeter) scales. However, few studies have undertaken extensive characterization of the complex biogeochemical processes at relevant sampling scales to describe transition zones.

Past field investigations have been limited by the difficulty in obtaining geochemical measurements at representative spatial scales to characterize the small and transient nature of interface zones (Hunt et al., 1997). The small volumes of fluid available for analytical measurements also limit the characterization of the organic and inorganic species involved in complex redox reactions (Christensen et al., 2000). Commonly used sampling methods, including well pumping and porewater extraction from sediment cores, raise concerns such as the potential mixing of waters from various zones and sediment disturbances. Water samples reflecting *in situ* equilibrium conditions at discrete intervals can be collected using passive diffusion samplers or "peepers" (Hesslein, 1976) to limit mixing with adjacent zones. One consequence of using peepers at 0.5–1 cm intervals is the small sample volumes obtained. Generally, sample volumes greater than 0.5 mL are required for common analytical techniques for inorganic and organic ions, such as ion chromatography,

atomic absorption, and gas chromatography. Using these techniques, the total volumes necessary for complete redox characterization cannot be obtained from cm-scale peepers. Capillary electrophoresis (CE), an emerging technology in environmental sciences, overcomes these volume limitations, by requiring very small sample volumes, ~1 nL per injection for a chemical suite with no preprocesseing (Linhardt and Toida, 2002). For example, all anionic parameters can be analyzed in triplicate with 10 μL of pipetted sample.

This paper presents a high-resolution biogeochemical study targeting the mixing interface zones within a wetland–aquifer system near the Norman Landfill in Norman, Oklahoma. The site is an ideal location for studying geochemical gradients because the wetland–aquifer system contains several shallow interfaces where waters of differing redox potential mix. The purpose of this paper is to document the biogeochemical gradients that result at these mixing interfaces and present appropriate field-laboratory methods to describe resulting gradients at sufficiently fine spatial resolution. Emerging CE technology to analyze environmental samples provides the ability to measure biogeochemical indicators on smaller volumes of fluid and thus allow investigations at smaller spatial scales. New knowledge of the importance of interface zones on biogeochemical cycling will allow for improved prediction of chemical fate and transport and assessment of natural attenuation of contaminated sites.

2. Background

2.1. Site description

The Norman Landfill, situated in the Canadian River alluvial plain in central Oklahoma (Fig. 1), was a municipal, non-restricted solid waste landfill that operated from 1922 to 1985 in the city of Norman, OK. The geologic setting is characterized by moderately permeable alluvial and terrace deposits with a shallow water table that overlies a Permian shale and mudstone confining unit known as the Hennessy Group (Scholl and Christenson, 1998). The reworked alluvium is about 12 m thick in the landfill area (Stacy, 1961) and the hydraulic conductivity is estimated to range from 7.3×10^{-2} to 2.4×10^{1} m/day (Scholl and Christenson, 1998). Leachate from the unlined landfill has resulted in a groundwater plume that extends downgradient approximately 250 m from the landfill toward the Canadian River and flows directly beneath the wetland (slough) (Scholl and Christenson, 1998). The wetland is likely a previous location of the main river channel, fed by groundwater discharge and precipitation. The wetland's water levels vary seasonally ranging from approximately 1 m deep in the spring to dry in the summer. Upper sediments have been variably saturated during the summer months.

The Norman Landfill has been designated as a U.S. Geological Survey research site under the USGS Toxic Substances Hydrology Program since 1995. It is the site of active, ongoing investigations into the biogeochemistry of the plume. Recent studies at the site by Lorah et al. (submitted for publication) targeting biogeochemical cycling within the wetland system demonstrate the spatial and temporal link between redox conditions in the wetland sediments and fluctuations in groundwater/surface water levels. Generally, during periods of high recharge, the upgradient bank of the slough had higher concentrations of leachate constituents including NH_4^+, dissolved organic C, Fe^{2+} and HCO_3^- in the top 60 cm of the wetland–sediment porewater compared to low recharge periods, indicating that leachate plume water from the aquifer discharged into the wetland. Scholl et al. (2005) also observed that exchange between the wetland and shallow groundwater was episodic and that shallow groundwater downgradient from the slough contained, on average, 29% wetland water during periods of high recharge. A generalized conceptual model showing the connection between the wetland (slough) and surrounding aquifer is shown in Fig. 2.

2.2. Core description

The surficial sediments of the wetland adjacent to the Norman Landfill consist of alternating units of fluvial silt and sand. The following description is based on the sequence of layers in a shallow core collected near the location of the peepers (Fig. 3).

2.2.1. Upper silt unit (0–40 cm)

The upper 40 cm of the core consists of organic-rich silt, referred to as the upper silt unit. The uppermost 10 cm of this unit contain abundant particulate organic matter, including plant fibers, seeds, insect parts and snail shells. The organic content of the upper silt unit decreases with depth (Fig. 4). Snail shells are most abundant in the top 25 cm of the upper silt unit, but occur sporadically

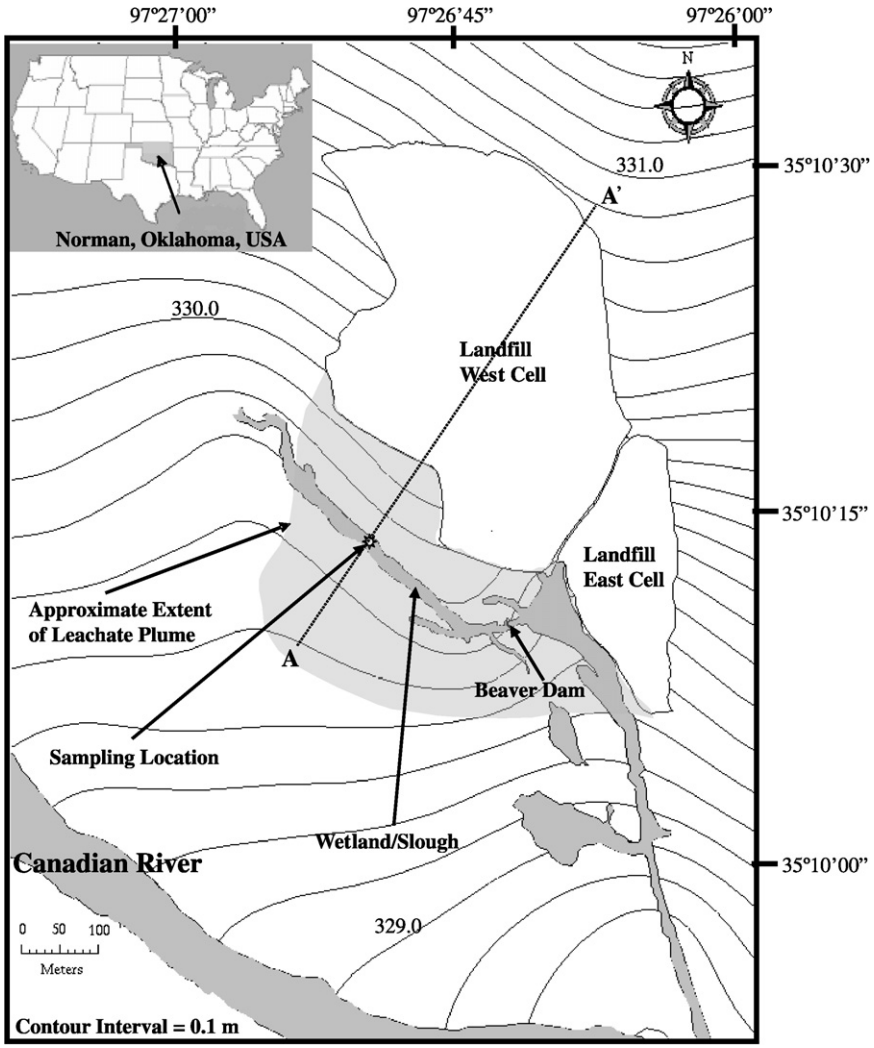

Fig. 1. Map of the Norman Landfill site in Oklahoma, US, showing the sample location. Modified from Scholl and Christenson (1998).

throughout the core. When exposed to light, seeds in the upper 18 cm of this unit sprouted. Seeds below 18 cm in the core did not sprout. The upper silt unit is laterally extensive and appears in all cores collected from the wetland (unpublished field data).

2.2.2. Transition zone (40–46 cm)

The next two units in the core together form a highly variable transition zone between the upper silt unit and the underlying coarse sand unit. The upper unit of the transition zone is a 3–4 cm layer of tan, medium to coarse-grained sand, referred to as the upper sand unit. The contact between the upper silt unit and the upper sand unit preserves relict burrows. The lower unit of the transition zone is a thin, organic-rich muddy silt unit, 2–3 cm thick, referred to as the middle silt unit. The contact between the upper sand and middle silt units is erosional.

2.2.3. Coarse sand unit (46–59 cm)

The middle fine-grained unit overlies a clean, grey, coarse-grained sand unit, 13 cm thick, referred to as the coarse sand unit. This unit is laterally extensive and the combination of coarse grain size and light grey color make it easy to identify in all cores collected from the wetland (unpublished field data). The contact between the middle silt unit (at the bottom of the transition zone) and the coarse sand unit contains relict burrows. No peeper data were collected below 52 cm in the coarse sand unit.

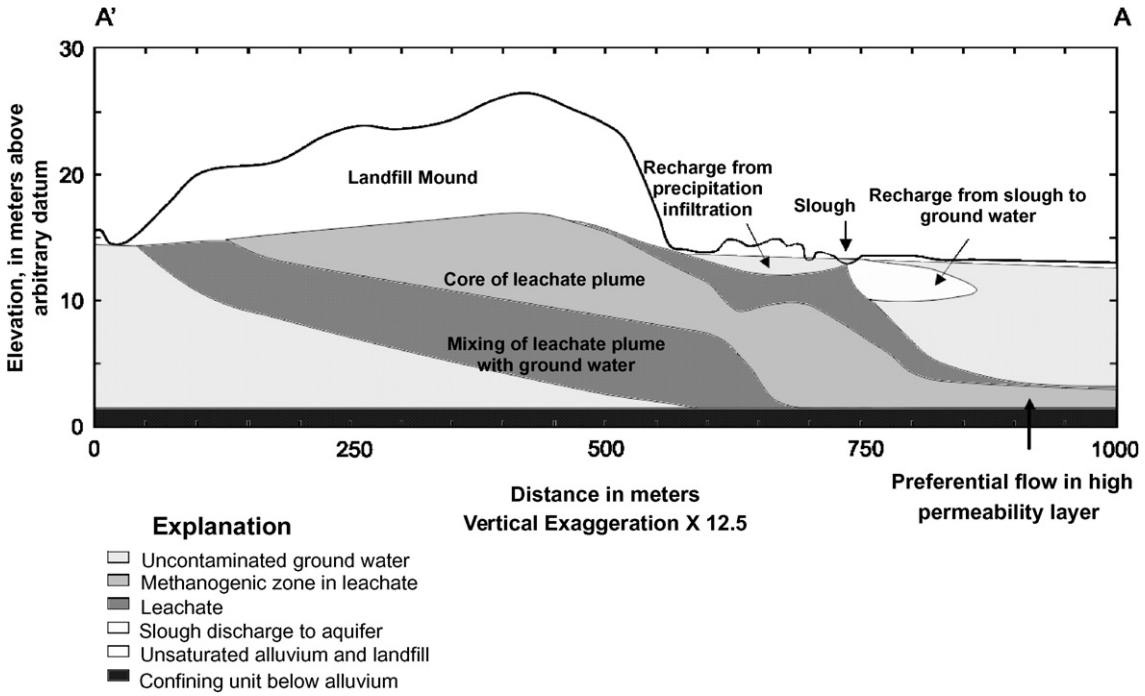

Fig. 2. Cross-sectional view of the Norman Landfill along section A–A′ (as shown in Fig. 1). The leachate plume and recharge zones are drawn on the basis of chemistry measurements made in the aquifer between 1997 and 2002 (from Scholl et al., 2005).

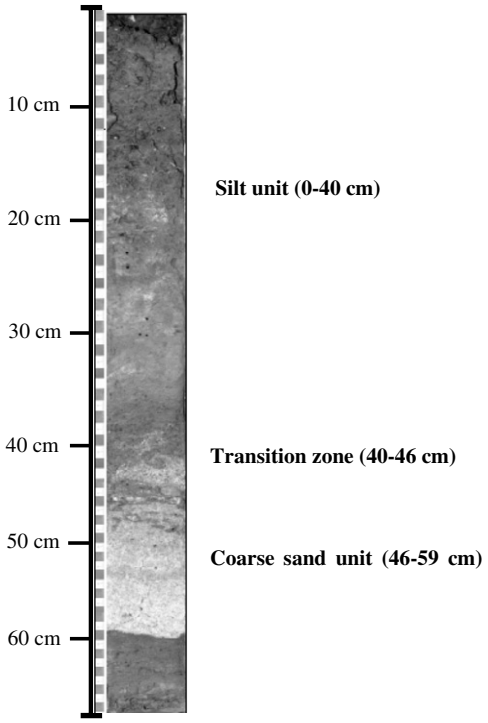

Upper silt unit - 0 to 40 cm (40 cm)

- 0-22 cm. Sediment is mostly silt and fine sand with organic material (green grasses, leaves and fibrous roots in the top 10 cm).
- 23-35 cm. Less organic material, some bioturbation.
- 36-39 cm. Fine sand and yellowish brown fine grains, burrowed contact with coarse sand below.

Transition zone:

Upper sand unit - 40 to 43-44 cm (3-4 cm)

- Uniform coarse sand. Erosional contact with middle fine grained unit.

Middle fine-grained unit - 43-44 cm to 46 (2-3 cm)

- Burrowed contact with middle sand unit.

Coarse sand unit - 46-59 (13 cm)

- Uniform coarse sand. Erosional contact with lower fine grained unit below.

Lower silt unit - 59-66 (7 cm)

- Very dark grayish brown silty mud. Erosional contact with sand below.

Fig. 3. Photograph of sediment core collected in 2004 near the peeper location. Description of sediment layers corresponding to depth.

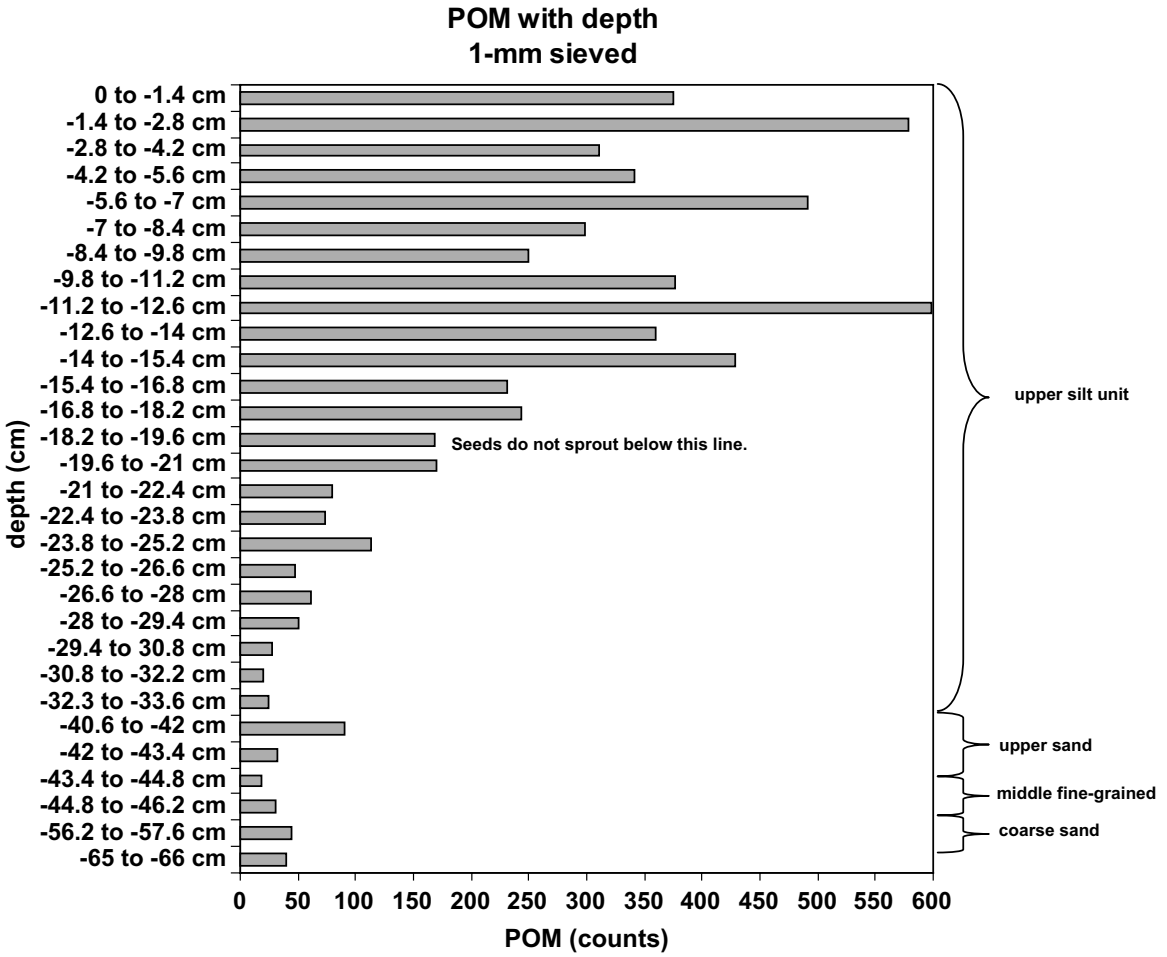

Fig. 4. Particulate organic matter (POM) counts from the >1 mm sieved fraction of the core shown in Fig. 3. Sand units yielded little or no POM, and therefore, not all sand units from the core were sieved and thus do not appear on this diagram creating a non-linear scale.

2.2.4. Lower silt unit (59–66 cm)

The coarse sand unit overlies an organic-rich silt layer, 7 cm thick, referred to as the lower silt unit. Like the coarse sand unit, the lower silt unit is laterally extensive and was observed in a core collected 5 m from the peeper (unpublished field data). The contact between the coarse sand layer and the lower silt unit is erosional.

2.2.5. Lower sand unit (66–76 cm)

At the bottom of this core, the lower silt unit appears to have overlain a sandy layer, which was not retained during extraction. In a core collected 5 m from the peeper (unpublished field data), the lower silt unit overlies a fine-grained sand layer referred to as the lower sand unit.

The silt/sand couplets in these cores record 3 depositional sequences. The coarse sand layers are interpreted as flood deposits and the overlying organic-rich silts as wetland sediments. One implication of this depositional interpretation is that sand units reflect rapid deposition during floods, whereas silt layers may have accumulated slowly over a series of years. The contacts between the sand units and the underlying organic-rich silt units are erosional; the contacts between the sand units and the overlying organic-rich silt units contain relict burrows indicating the influence of aquatic invertebrates (probably crayfish).

3. Materials and methods

3.1. In situ measurements

Water samples were collected during the "wet" spring season in May 2003 from the wetland adjacent

to the Norman Landfill using peepers (Hesslein, 1976). Two peepers with 0.45-μm Millipore® membrane were used to obtain vertical profiles of surface water, porewater and groundwater with a 0.5–1 cm resolution. The peepers have a total of 37 horizontal ports in which, the first 22 ports have apertures and spacing of 0.5 cm followed by 15 ports with apertures and spacing of 1 cm. The peepers span a vertical profile 52 cm deep. This peeper design allows discrete water samples to be obtained at small spatial resolution by limiting the vertical mixing of adjacent water masses during sampling.

Peeper ports were filled with nanopure water (18 mΩ) and deoxygenated with N_2 for 3 days to remove O_2 from the water and plastic samplers. Peepers were then transported in an anaerobic PVC-constructed chamber to the site and maintained under deoxygenated conditions until insertion into the wetland sediments. The peepers were positioned in the wetland for 2 weeks (April–May 2003) to allow equilibration and diffusion of solutes between the nanopure water and surrounding porewater (Azcue et al., 1996; Jacobs, 2002; Webster et al., 1998). The peepers were positioned 40 cm apart in the center of the wetland parallel to groundwater flow at two different depths. In peeper 1 the first 21 cm sampled the water column and the next 29 cm sampled the sediment porewater. Peeper 2 was buried completely in the sediments capturing the sediment porewater down to a depth of 52 cm below the sediment–water interface (0 cm). After 2 weeks of equilibration, the peepers were retrieved and processed immediately in an anaerobic glove bag filled with a N_2 atmosphere.

From the peeper ports, 12 mL of sample were obtained of which 2 mL were used for the analysis of alkalinity, 2.5 mL for dissolved Fe(Fe^{2+}) and 3 mL for H_2S, which were measured in the field using methods of electrometric Gran titration and colorimetric spectroscopy modified for low sample volumes (APHA, 1975; AWWA et al., 1971). For laboratory analyses, including cations, anions, organic acids and NH_4^+, 1 mL of water was collected which was greater than needed. Cations were preserved in 1% trace metal grade HCl, anions were preserved in 0.5% formaldehyde, organic acids and NH_4^+ were flash-frozen with dry ice and stored for laboratory analysis. Dissolved O_2, pH, conductivity, temperature and redox potential were measured at the wetland using a 600 XLM YSI Hydrodata multiparameter meter (Yellow Springs, OH, USA).

3.2. Capillary electrophoresis analyses

An Agilent Technologies capillary electrophoresis (CE) instrument with a photo diode array detector was used for the analysis of anions (SO_4^{2-}, Cl^-, NO_3^-, NO_2^-), cations (Ca^{+2}, Mg^{+2}, K^+, NH_4^+, Na^+), and low molecular weight organic acids (acetate, butyrate, oxalate, lactate, propionate). For all of the analyses a 56 cm long fused silica capillary with 50 μm I.D. and an extended path length of 150 μM at the detection window was used. Tapered polypropylene vials were filled with ~30 μL of sample, more than sufficient volume for multiple replicate runs. The samples were injected by hydrostatic pressure followed by a 2 s injection of the electrolyte chosen for each analysis (each injection consumed ~1 nL/sample). The temperature was held constant at 25 °C. Table 1 shows the conditions for each analysis.

3.3. Saturation indices

Mineral equilibria were evaluated using saturation indices (SI) calculated with the program PHREEQC-2 (Parkhurst, 1995) and the PHREEQC database. All measured inorganic species were included in the speciation model as were pH and an approximate temperature of 15.9 °C deduced from the measured temperature of the bottom waters. Due to the high concentrations of organic acids found in the system, the alkalinity values obtained from Gran titration (i.e., the total acid neutralizing capacity (ANC)) were corrected for the contribution of organic acids. It has been demonstrated that small chain organic acids contribute to the total titrated alkalinity (Baedecker and Cozzarelli, 1992; Devlin, 1991; Hemond, 1990), and thus uncorrected field data may overestimate HCO_3^- concentrations. Although previous studies have shown a complex relationship between observed alkalinity and organic acid concentration, Baedecker and Cozzarelli (1992) demonstrated that acetate contributed linearly to alkalinity in well-buffered solutions with HCO_3^- concentrations of 100 microequivalents. Thus, in the high HCO_3^- system of the Norman Landfill wetland, a reasonable correction would be to assume that the low molecular weight organic acids detected in these waters (acetate, propionate, butyrate) were titrated in the field. Field alkalinity values were corrected by subtracting the sum of the milliequivalents of acetate, propionate, and butyrate and the remaining alkalinity

Table 1
Capillary electrophoresis setup conditions for the analysis of major ions

CE conditions	Analytes		
	Cl^-, Br^-, NO_3^-, NO_2^-, and SO_4^{2-}	Ca^{2+}, Mg^{2+}, Na^+, K^+ and (NH_4^+)[a]	Formic, acetic, propionic, and butyric acids
Buffer solution	Chromate electrolyte solution from Waters Corp.	Ionphore cation DDP electrolyte buffer concentrate from Dionex Corp.	Chromate electrolyte solution from Waters Corp.
Sample detection			
Wavelength, bandwidth (nm)	325, 10	450, 80	315, 20
Reference detection			
Wavelength, bandwidth (nm)	375, 40	230, 20	375, 40
Voltage (kV)	10	20	10
Current (μA)	14	300	14
Hydrostatic injection	35 mbar: 2 s with electrolyte 15 s with sample 2 s electrolyte	50 mbar: 0.1 s with sample 2 s with electrolyte	35 mbar: 15 s with sample 2 s with electrolyte
Duration of run (min)	15	10	12
Conditioning between sample runs	5 min water 5 min 0.1 N NaOH[b] 5 min electrolyte solution	5 min water 5 min electrolyte solution	3 min water 3 min 0.1 N NaOH[b] 5 min electrolyte solution
Dilution	No dilution	1:10	1:10

[a] Samples were not diluted and the sample injection time was 1 s.
[b] One disadvantage with this method is the use of a NaOH flush between runs. This was added to eliminate memory effects but resulted in rapid degradation of the interior of the fused silica capillaries and thus should be avoided if possible. Other possible rinses to avoid memory effects include using sodium borate or sodium phosphate adjusted to a pH of 9.

was assumed to be HCO_3^-. These corrected values were included in the PHREEQC input files used to generate the saturation indices to determine mineral equilibria. It should be noted that a comparison of the SI for calcite, siderite and mackinawite calculated with corrected and uncorrected alkalinities show that the values were only minimally affected (e.g., ~0.1 lower for calcite), even for the samples with the highest observed organic acid concentrations.

4. Results

4.1. Wetland surface water description

The shallow surface water, ~1 m, was found to be stratified with respect to water parameters such as temperature, redox potential (ORP), O_2 levels, and pH (Table 2). A dense layer of aquatic grasses was observed covering the surface water at the end of April 2003 when the peepers were placed in the sediments. At this time, the water column was found to be stratified with high levels of dissolved O_2 at the top of the surface water (covered by grasses) and high pH presumably due to high levels of photosynthesis. Below the plant cover, the O_2 concentrations and pH decreased. In May 2003, when the peepers were retrieved, the vegetation was decaying and the bottom water was anoxic and free of NO_3^-.

Table 2
Parameters of the water column at the time of peepers' insertion

Water column	Temperature (°C)	pH	Dissolved oxygen (mg/L)	Specific conductivity (μS/cm)
Surface	19.50	8.13	~15.50[a]	1578
Bottom	15.86	7.21	3.09	1742

[a] Measurements taken near photosynthesizing plants and system was out of equilibrium. Reading did not stabilize.

4.2. Sulfur

Dissolved SO_4^{2-} concentrations were high in the water column with a maximum of 646 μM (Fig. 5). A significant decrease in concentration was observed at the sediment–water interface (0 cm depth, Fig. 5) from 584 μM to 15.0 μM across a 4 cm interval. This decrease in SO_4^{2-} at the sediment–water interface is spatially concurrent with an increase in H_2S (Fig. 5). Hydrogen sulfide concentrations were highest at the sediment–water interface (1004 μM) and were, on average, 5.7 times

higher in the water column than in the sediments. Within the sediment profile (−1 to −28 cm), SO_4^{2-} concentrations were low and remained relatively constant (fluctuating from 12 μM to 15 μM), and the average H_2S concentrations were 3 times higher than SO_4^{2-} concentrations (Fig. 5). Below −29 cm, SO_4^{2-} decreased sharply to levels below detection limits (<5 μM) while sulfide showed a gradual increase to a maximum of 257 μM just below the transition to the coarse sand unit (∼−46 cm).

4.3. Iron

In the water column, Fe^{2+} concentrations were low, with an average of 5 μM (Fig. 5) except for one locally reduced zone at 14 cm above the sediment–water interface, where Fe^{2+} values were 100 μM. At the sediment–water interface, Fe^{2+} concentration increased steeply coincident with the sharp decrease in SO_4^{2-} (Fig. 6). With increasing depth in the sediments, Fe^{2+} generally decreased ranging from 869 μM to 39.0 μM (at −5 to −52 cm). In the upper sediments (−1 to −28 cm), Fe^{2+} concentrations were 46 and 15 times higher than the concentrations of SO_4^{2-} and sulfide, respectively. Below −30 cm, dissolved Fe concentrations decreased to the lowest values, concomitant with increased sulfide concentrations.

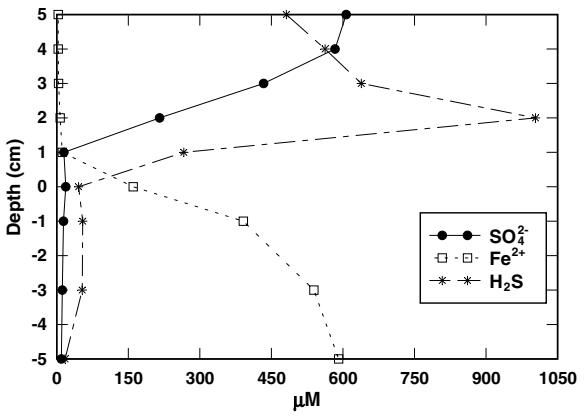

Fig. 6. Enlarged profile from depth 5 cm to −5 cm showing the concentrations of sulfate, iron(II) and hydrogen sulfide from Peeper 1 at the sediment–water interface (zero depth).

4.4. Nitrogen

Concentrations of NO_3^- and NO_2^- were both below detection limits (9.7 and 13.0 μM, respectively) in all samples for both peepers. Elevated NH_4^+ concentrations were found throughout the depth profile and showed significant gradients related to mixing interfaces (Fig. 5). At the sediment–water interface (0 cm depth), the NH_4^+ gradient reached a concentration of 14.8 mM over 3 cm. Similarly, a second maximum of 36.3 mM is

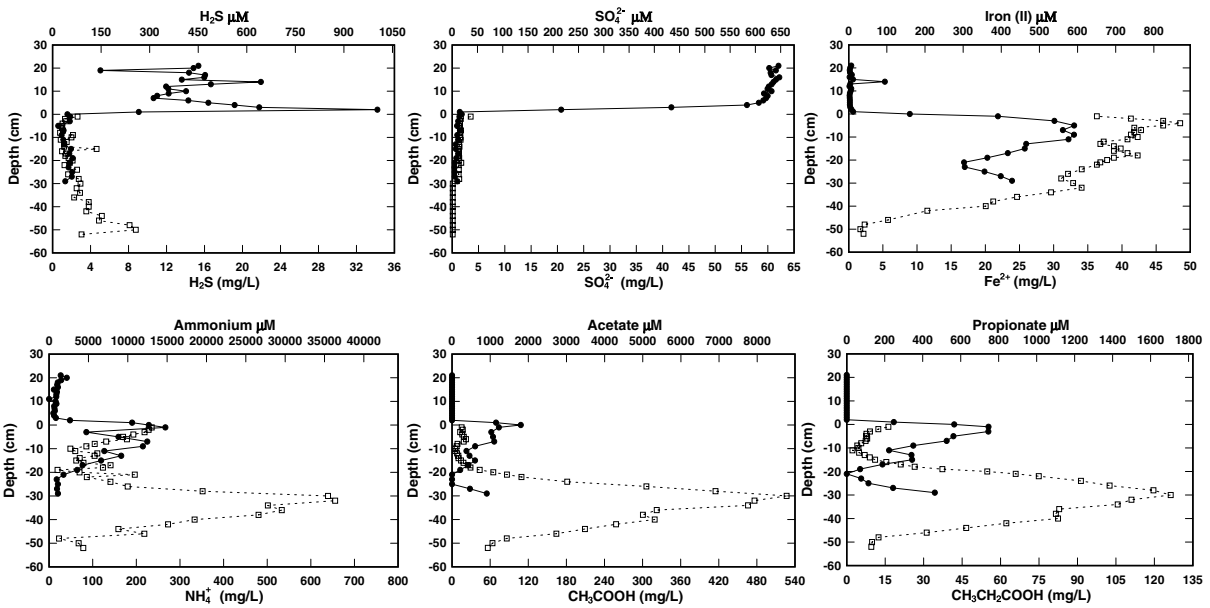

Fig. 5. Depth profiles for chemical concentrations. A depth of zero represents the sediment–water interface. Peeper 1 filled circles, peeper 2 empty squares.

observed at −32 cm over a spatial interval of ~5 cm. This peak occurs in the lower portion of the upper silt layer just above the transition zone to the coarse sand.

4.5. Organic acids

Waters were analyzed for acetate, butyrate, propionate, oxalate and lactate. Oxalate and lactate were not detected anywhere in the profile. The trends for acetate, butyrate and propionate were similar, although the concentrations were greatest for acetate (Fig. 5). The sharp concentration gradients of organic acids were similar to those observed for NH_4^+. At the sediment–water interface, a peak in organic acids was observed; acetate reached a high concentration of 1.80 mM, propionate 0.75 mM and butyrate 0.08 mM. A second peak of elevated organic acid concentrations coincides with the location of the NH_4^+ peak (Fig. 5) in the lower portion of the upper silt layer just above the transition zone to the coarse sand. Here acetate reached a high concentration of 8.8 mM, and propionate and butyrate reached 1.7 mM. In the coarse sand layer, acetate decreased to a minimum of 0.94 mM, propionate to 0.13 mM, and butyrate to 0.074 mM.

4.6. Cl, cations, pH and alkalinity

Chloride concentrations gradually increased with depth (Fig. 7) in both peepers but the overall concentrations were higher in peeper 2 than peeper 1. In peeper 1, the lowest concentration of Cl^-, ~1.8 mM, was observed in the surface water. Chloride concentrations, increased in the sediments to a maximum of 3.5 mM at 29 cm depth. Concentrations in Peeper 2 were 5.1 mM in the upper silt layer and gradually increased to a maximum of 7.4 mM in the coarse sand layer (Fig. 7).

The pH was highest in the water column (~8.5) and decreased sharply to ~7.5 at the sediment–water interface coincident with the decrease of SO_4^{2-}. In the upper silt layer the pH values were noisy and have a minimum (~6.9) at approximately the same location as the high concentrations of organic acids (~30 cm) (Figs. 5 and 8). The alkalinity profile shows an oscillating pattern with an average concentration of 15 mM in the water column (Fig. 8). Within the first 5 cm of the upper silt layer, alkalinity concentrations increased to a maximum of 35 mM. Below this point, oscillating concentrations decreased to 22 mM at ~30 cm and fluctuated between 16 mM and 25 mM below this depth (Fig. 8).

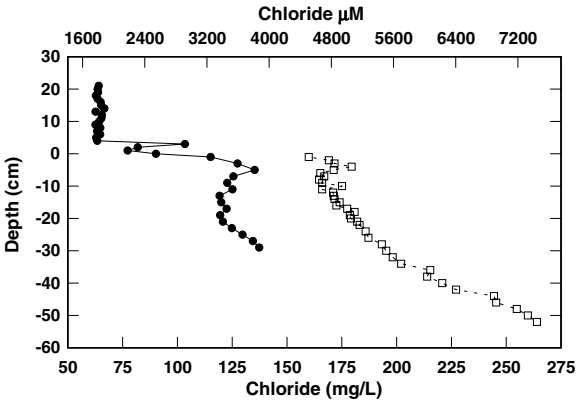

Fig. 7. Depth profile for chloride. A depth of zero represents the sediment–water interface. Peeper 1 filled circles, peeper 2 empty squares.

Cation concentrations showed similar cm-scale oscillations and were higher in the water column than in the porewater, with a maximum of 31 mM Ca^{2+} (Fig. 8), 12 mM Mg^{2+}, 2.2 mM K^+ and 19 mM Na^+ (data not shown). The highest levels of Ca^{2+} were observed in the upper portions of the water column near the dense aquatic grasses. Saturation indices (SI) suggest that the entire profile was supersaturated with respect to calcite with average SI values in the water column of 2.3, 1.8 in the upper silt layer, 1.7 in the transition zone, and 1.5 in the coarse sand layer (Fig. 8). Saturation indices indicate that the water column was undersaturated with respect to siderite, except at 14 cm above the sediment–water interface with an SI of 0.8. The sediments are supersaturated with respect to siderite with values oscillating between 1.6 and 3.0 above 45 cm depth. Below 45 cm depth, SIs decreased to 0.3 (profile not shown).

5. Discussion

5.1. Wetland–aquifer system

Chloride is a non-reactive anion and has been found to be a good tracer for the presence of water impacted by landfill leachate (Grossman et al., 2002; Röling et al., 2001; van Breukelen and Griffioen, 2004). An observed gradual increase of Cl^- with depth suggests transport from the underlying landfill leachate into the wetland (Fig. 7). Both peepers show a similar trend but higher concentrations were observed in peeper 2, which was ~40 cm closer to

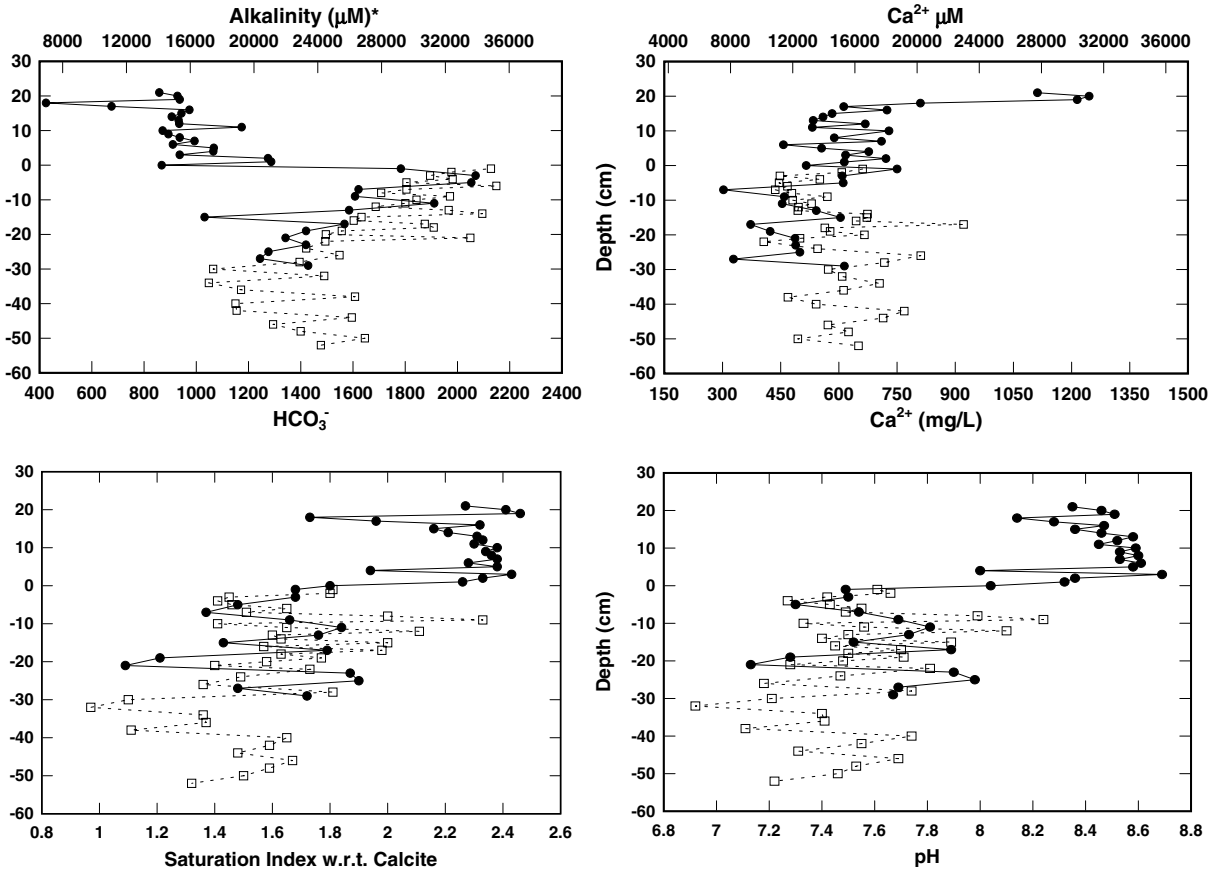

Fig. 8. Depth profiles for alkalinity, pH, calcium and saturation index with respect to calcite. A depth of zero represents the sediment–water interface. Peeper 1 filled circles, peeper 2 empty squares. *Alkalinity concentrations corrected for the effect of organic acids (See Section 3.3).

the upgradient bank of the wetland. Overall concentrations of Fe^{2+} were also higher in peeper 2 perhaps due to the presence of higher concentrations of Fe leached from the landfill to be recycled. Because of the reactive nature of Fe the trends in Fe^{2+} do not match the trends in Cl^- but suggest that over time the effects of the landfill leachate can be seen in the wetland porewater.

5.2. Sulfate, hydrogen sulfide and iron

The wetland was anoxic and NO_3^- was absent, making Fe and SO_4^{2-} reduction the most favorable TEAPs at the sediment–water interface. The decrease in SO_4^{2-} observed at the sediment–water interface (depth 0 cm, Fig. 5) is attributed to bacterial SO_4^{2-} reduction as SO_4^{2-} is considered chemically to be metastable at standard earth surface temperatures (Nealson, 1997). Sulfate is utilized by SO_4^{2-}-reducing bacteria as an electron acceptor, and is reduced to H_2S to drive metabolism. Because SO_4^{2-} reduction was occurring in the loose "fluffy" bottom sediments at the sediment–water interface, it is likely that the sulfide produced was diffusing upward into the water column as observed in the sulfide profile (Fig. 5). Hydrogen sulfide speciation was evaluated and shows that H_2S existed as an ion and not as a dissolved gas. Sulfide concentrations remained high due to the hypoxic nature of the water column (Table 2). This is common in meromictic lakes where an oxic/hypoxic stratification in the water column is permanent and H_2S diffuses from the bottom sediments into the water column causing a depletion of O_2 (Ciglenecki et al., 2005).

In the sediments, sulfide was present in lower concentrations than in the water primarily due to its high reactivity with Fe^{2+} to form Fe sulfides. Saturation indices suggest that the system is supersaturated with respect to mackinawite throughout the profile with higher SIs below the sediment–water

interface (2.7–4.1) suggesting that the system precipitated iron sulfides. Iron sulfide minerals including pyrite have been observed at the Norman Landfill site (Breit et al., 2005) and similar environments (Adler et al., 2000; Koretsky et al., 2003). A Spearman's Rank Order Correlation Analysis reveals that sulfide exhibits a significant negative correlation with Fe^{2+} ($r_s = -0.809$, $n = 73$, $p < 0.01$) throughout the profile.

Dissolved Fe in the sediments is a product of the reduction of Fe(III) in various forms by abiotic and/or biotic processes. In freshwater aquatic sediments and groundwater at near neutral pH, biotic processes are more important in the reduction of Fe(III) than abiotic processes (Lovley et al., 1991). Thus, high concentrations of Fe^{2+} are likely a consequence of the activity of Fe reducers. In addition, the system was supersaturated with respect to siderite. Previous studies have reported waters supersaturated with respect to siderite and authigenic siderite formation in aquifers with active Fe reduction (Baedecker et al., 1993; van Breukelen et al., 2004). Examining the profiles in Fig. 6, an increase in Fe^{2+} is observed just below the decrease in SO_4^{2-}, near the sediment–water interface. This suggests that either SO_4^{2-} reduction was occurring above Fe reduction in the sediments or SO_4^{2-} and Fe reduction were occurring in the same location but Fe^{2+} is not observed due to precipitation with sulfide. This could be explained by the high concentrations of organic matter at the sediment–water interface and heterogeneities in the phases of Fe oxides being utilized. A study by Cozzarelli et al. (1999a) demonstrated simultaneous occurrence of Fe and SO_4^{2-} reduction for an aquifer contaminated with gasoline. Other studies have documented concurrent dynamics between Fe and SO_4^{2-} reducers. For example, in an acidic lake the availability of SO_4^{2-} exceeded the availability of reactive Fe causing the SO_4^{2-} reducers to outcompete the Fe reducers (Blodau et al., 1998). They found that SO_4^{2-} and Fe reduction occurred simultaneously but higher energy yields were obtained from SO_4^{2-} reduction than from Fe reduction. The result was attributed to low concentrations of bioavailable oxidized Fe even though the sediments contained high concentrations of other oxidized Fe species. Another study found Fe reducers and SO_4^{2-} reducers existing actively in the same localized zone (Motelica-Heino et al., 2003). The most unstable Fe oxides will be consumed preferentially and the remaining Fe oxides become refractory allowing for SO_4^{2-} reduction. In systems where Fe oxides of different stability are present, the boundaries between the zones of Fe and SO_4^{2-} reduction are more diffuse (Postma and Jakobsen, 1996). In the system discussed here, the wetland has high concentrations of SO_4^{2-} for a freshwater system, likely due to dissolution of gypsum naturally present in the Permian rocks (Ulrich et al., 2003) and heterogeneous quantities of Fe have been found at the site (Cozzarelli et al., 1999b) with low concentrations of bioavailable Fe (Breit et al., 2005). Most of the detectable Fe(III) in the aquifer sediments was associated with clays and was very slow to react during reductive dissolution. The reduction of the ferric oxides present in the clay particles was interpreted to be diffusion limited (Breit et al., 2005). These conditions could allow simultaneous redox reactions at the sediment–water interface. Evidence of the coexistence of Fe and SO_4^{2-} reduction was also observed at 14 cm above the sediment–water interface with 100 μM Fe^{2+} and 638 μM sulfide (Fig. 5). These peaks likely represent a localized microzone of anaerobic conditions driven by dense suspended organic material including decaying aquatic grasses. In addition to providing organic matter, the grasses in the water column may also serve as a structure on which solid phase Fe oxide particles may be present.

With depth in the wetland sediments, the Fe and S cycles are linked and trends correlate well to transitions between sedimentary layers (Fig. 9). Sulfate concentrations were relatively constant with depth (poised at ~15 μM) until 30 cm when a sharp decline to levels below detection limit is observed. Interestingly, changes in SO_4^{2-} do not correlate well with changes in sulfide concentrations (e.g., peaks in sulfide correspond to zones with low/no free SO_4^{2-}). In zones with low/no free SO_4^{2-}, observed sulfide is interpreted to be from either transport processes (i.e., upward movement from the sand layer) or *in situ* SO_4^{2-} reduction where SO_4^{2-} reducing bacteria are utilizing barite as a SO_4^{2-} source as has been previously demonstrated at the site (Ulrich et al., 2003). It is interesting to note that an increase in H_2S (and decrease in Fe^{2+}) occurred below 18 cm, the same boundary where seeds were no longer viable and the particulate organic matter concentrations decreased (Fig. 4). Hydrogen sulfide is generally considered to be toxic to wetland plants (Koch et al., 1990) and may affect seed viability. The increase in H_2S observed in the coarse sand layer (Fig. 9), may represent an increase in SO_4^{2-} reduction

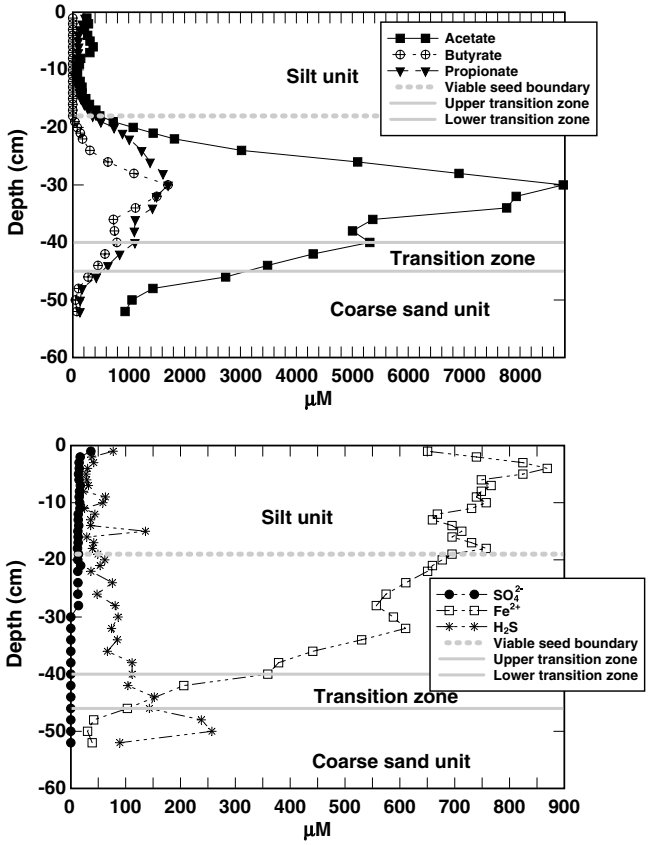

Fig. 9. Comparison of profiles at peeper 2 for organic acids (top), sulfate, dissolved iron and sulfide (bottom) showing the linkages to the sedimentary units. A depth of zero represents the sediment–water interface.

rates or simply loss of Fe^{2+} from the system through precipitation.

5.3. Organic acids

Concentrations of organic acids throughout the sediment profile result from the activities of fermentative bacteria (Capone and Kiene, 1988; McMahon and Chapelle, 1991). Decomposition of organic material in anaerobic environments requires a consortium of organisms. The fermentative bacteria transform organic substrates to low molecular weight organic acids and H_2, which act as electron donors for various terminal electron accepting processes (Ho et al., 2002). Many fermentation products have been studied as indicators of organic C decomposition (Ho et al., 2002) and microbial activities (Boschker et al., 1998; Kleikemper et al., 2002). Other studies emphasize the importance of fermentation products on remediation of contaminated subsurface systems (Aulenta et al., 2005). A build-up of organic acids implies that their production exceeds consumption at that location. For example, McMahon and Chapelle (1991) observed that fermentative products were present in greater abundance in aquitard than aquifer sediments related to the availability of electron acceptors.

In this study, high concentrations of fermentation products were found at the sediment–water interface and in the lower portion of the upper silt layer just above the transition zone to the coarse sand. The build-up in organic acids (acetate, propionate and butyrate) at the sediment–water interface is attributed to decomposition of organic material from the wetland, such as plant biomass (Kostka et al., 2002). The decay of aquatic grasses provides a source of organic C and is likely the trigger for the anaerobic conditions in the surface water. Elevated concentrations of labile organic matter at the sediment–water interface provide the electron donors for Fe and SO_4^{2-} reduction.

The source of the high concentration of organic acids observed above the transition zone (20–42 cm) is uncertain. One possible source is the

decomposition of a localized concentration of organic matter. Although, the overall trend of the particulate organic matter found in the core (Fig. 4) shows a decrease with depth, this does not exclude the possibility that a local organic concentration exists near the peepers given the heterogeneity of the macrobiology in the system. Another possibility is that the organic acids originate from degradation of DOC from the leachate plume. Discharge from the aquifer into the wetland during recharge periods can be a source of DOC to the wetland sediments (Lorah et al., submitted for publication). The gradual increase in Cl^- concentrations with depth supports that leachate components have migrated upward into the wetland. However, the highest concentrations of DOC (160 mg/L) found in the leachate-contaminated aquifer upgradient from the wetland (Eganhouse et al., 2001) are much lower than the sum of organic acids observed in this study. A likely scenario is that both natural DOC from buried organic matter in the wetland and DOC from leachate contribute to the high acetate concentrations observed.

Below ~18 cm, concentrations of organic acids increase reaching a maximum at ~30 cm due to the low availability of electron acceptors. This is supported by other studies that have shown steep gradients in organic acids associated with abrupt changes in biological activity due to changes in the supply of electron acceptors, temperature, supply of labile organic C, or shifts in methanogen population (Cozzarelli et al., 1994; Ho et al., 2002; Shannon and White, 1996). Acetate concentration reaches 8800 μM, which is 4 times higher than the peak at the sediment–water interface and higher than levels reported in the literature (Fig. 9). Studies in diverse sedimentary environments report acetate concentrations such as, 1000 μM in peat bogs (Duddleston et al., 2002; Shannon and White, 1996), 1200 μM (Kostka et al., 2002) and 1600 μM (Hines et al., 1994) in salt-marsh sediments, 60 μM (McMahon and Chapelle, 1991) and 500 μM (McMahon, 2001) in aquifer–aquitard sediments, 25 μM in estuarine sediments (Wellsbury and Parkes, 1995), and 10 μM in marine environments (Ho et al., 2002). However, in petroleum deposits low molecular weight organic acids can reach higher concentrations up to 166,500 μM (10,000 mg/L for acetate) (Kharaka et al., 1993).

In addition to finding a steep gradient of organic acids in the upper silt layer, the shape and location of this gradient is also interesting (Fig. 9). The steep increase in organic acids at 18 cm coincides with the maximum depth of seed viability in the core and with decreased levels of coarse particulate organic matter (Fig. 4). Loss of seed viability may be a response to increased levels of organic acid in the porewater, as well as increased levels of H_2S (see Section 5.2). Crop residues have been shown to inhibit seed germination in fields due to high levels of phenolic acid in the soil (Sène et al., 2000). However, almost no data exist on the link between seed viability and the abundance of simple organic acids in wetland soil. The steep increase in organic acids may also signal a change in the quality of particulate organic matter below 18 cm. This is the focus of ongoing studies.

5.4. Ammonium and nitrate

Thermodynamics suggest that NO_3^- will be one of the first alternate electron acceptors to be utilized by anaerobic bacteria in anoxic aquifers. Nitrate was below detection limits throughout the profiles suggesting that any available NO_3^- has been consumed and less thermodynamically favorable processes (e.g., SO_4^{2-} reduction) dominate. The primary N species in the system is NH_4^+ which originates from both active microbial cycling of wetland organic matter and transport from the landfill leachate plume. Elevated NH_4^+ concentrations were found throughout the sediment profile (Fig. 5) but generally follow the same trend as acetate, propionate, and butyrate with maximum concentrations at the sediment–water interface and −30 cm depth suggesting a similar source (see Section 5.6). The correlation of NH_4^+ and organic acids is consistent with mineralization of organic matter as noted in other studies (Bally et al., 2004). The high levels of NH_4^+ together with lower pH and higher alkalinities suggest significant organic matter degradation.

5.5. Cations and alkalinity

The alkalinity profile is controlled by TEAPs and mineral precipitation/dissolution reactions. Iron and SO_4^{2-} reduction increase alkalinity whereas methanogenesis decreases alkalinity (Schlesinger, 1997). In the surface water, alkalinities are lower with the exception of a peak at 14 cm above the sediment water–interface where other TEAP indicators suggest Fe and SO_4^{2-} reduction. At the sediment–water interface, a sharp increase in alkalinity is consistent with the sharp increase in Fe^{2+} and decrease

in SO_4^{2-}. These trends support the interpretation of active SO_4^{2-} and Fe reduction at 14 cm and at the sediment–water interface. With depth in the sediments, alkalinities decrease as a result of CO_2 reduction likely by methanogenesis and possible precipitation of carbonate minerals including calcite and siderite. The surface water is undersaturated with respect to siderite with the exception of 14 cm (SI = 0.8) and within the silt unit, siderite SIs increase to 2–3 suggesting the system favors precipitation of siderite, which will decrease alkalinity. Saturation indices indicate that the system is supersaturated with respect to calcite (Fig. 8), however, the extent to which calcite is precipitating is unclear. Calcium concentrations are unusually high throughout the profile (highest concentrations observed in the upper water column near the aquatic grasses, see Section 5.6). These values may be explained by the high concentrations of organic C present in the system. Dissolved organic compounds and humic acids have been shown to inhibit calcite precipitation (Reynolds, 1978) and may explain the system being out of equilibrium.

5.6. Vegetation effects

Aquatic plants floating in the wetland provide an O_2 source to the surface water via photosynthesis. Oxygen levels (~15.9 mg/L) within the top 10 cm of the surface water are supersaturated (theoretical saturation at 20 °C is 10.9 mg/L). Measurements were taken from waters in contact with the aquatic vegetation and high concentrations are attributed to active photosynthesis. Senescence of the thick layer of aquatic grasses leads to decomposition of organic matter coupled to the depletion of O_2 and other electron acceptors. Jones et al. (2003) suggested that the redox gradient from oxic to anoxic conditions in the water column is influenced by the dynamic activity of aquatic plant cover. The random distribution of aquatic vegetation in the system resulted in microzones of reducing conditions within the water column as evidenced by (1) the increase in NH_4^+ and decrease in SO_4^{2-} at 20 cm above the sediment–water interface and (2) elevated sulfide and Fe^{2+} concentrations at 14 cm above the sediments.

The input of organic matter from decomposing plants provides abundant electron donors at the sediment–water interface for Fe and SO_4^{2-} reduction. Previous studies found an increase in SO_4^{2-} reduction rates when a wetland was covered with vegetation (Hines et al., 1989; Koretsky et al., 2005) and demonstrated the influence on redox stratification in the sediments to be more pronounced in the summer than in the winter due to vegetation dynamics (Koretsky et al., 2005).

Calcium carbonate dynamics also appear to be linked to the vegetation in the wetland system. In the upper portion of the water column, where aquatic grasses are abundant, Ca^{2+} concentrations and calcite SI were at their highest (~31 mM and 2.4, respectively). This is consistent with the possibility that grasses are playing a role in the cycling of $CaCO_3$ in the system. Some aquatic grasses such as sago pondweed precipitate $CaCO_3$ on their leaves, stems and lacunae which can be released to the water upon senescence (Kantrud, 1990).

5.7. Scale considerations

The potential effect of collecting samples at a larger spatial resolution than the cm-scale used in this study was evaluated numerically using the acetate concentrations measured in Peeper 2 as an example. The concentrations of acetate that would have been observed had samples been collected at intervals of 5 cm or 10 cm (C_w) were calculated by

$$C_{\mathrm{w}} = \frac{\sum Vk_i Ck_i}{\sum Vk_i}$$

where Ck_i is the actual acetate concentrations measured at 1 cm intervals and Vk_i is total volume associated with that concentration. Results show that if samples were collected at 5 cm intervals, the general trend would be the same but the maximum concentration observed would be ~78% of that observed using 1cm sampling (Fig. 10). The use of an even larger sampling interval, 10 cm, results in a substantially different concentration profile with the location of the maximum concentration being shifted ~7 cm lower than the peak concentration shown in the 1 cm profile. In addition, at −30 cm depth, the acetate concentration predicted from the 10 cm sampling interval would be ~60% of that shown in the 1 cm profile (Fig. 10). This exercise illustrates the significant impact that the scale of the sampling interval has on the observable concentration profiles in heterogeneous systems such as this.

Sampling at discrete 0.5–1 cm intervals was sufficient to resolve steep gradients observed (1) within the water column (e.g., 0.5 cm peaks in Fe^{2+} and H_2S at 14 cm above the sediment–water interface),

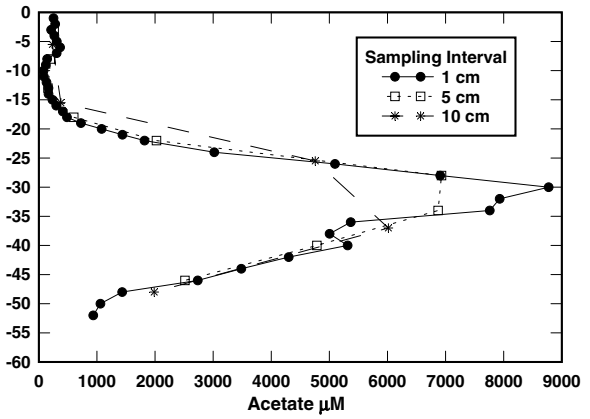

Fig. 10. Model of acetate concentrations by increasing the sample scale (5 and 10 cm) compared to the acetate concentrations obtained from peeper 2 (1 cm).

(2) at the sediment–water interface (e.g., decrease in SO_4^{2-}/increases in H_2S and Fe^{2+} over 4 cm), (3) at major lithologic boundaries within the sediment (e.g. decrease in organic acids in the transition zone to the coarse sand layer), and (4) within the sediment not associated with major lithologic contacts (e.g., ~20 cm peak in organic acids at 30 cm depth within the silt unit; oscillations of carbonate chemistry over 3–4 cm intervals). Although the microbiological processes controlling these gradients likely occur at a smaller (μm) scale, it is clear that resulting chemical dynamics can be resolved at the cm-scale in this system. This suggests that the combined use of small-scale peepers to collect discrete field samples and capillary electrophoresis to conduct complete geochemical analyses on limited sample volumes is a powerful technique for providing new insights into redox dynamics.

CE technology is becoming popular in environmental studies due to the wide arrange of chemical compounds that can be analyzed even in complex matrices. Some of the applications of CE include: analysis of organic acids in water and air (Dabek-Zlotorzynska et al., 2005; Huang et al., 2005; Wu et al., 2003), analysis of pesticides and pollutants in environmental waters (Frías et al., 2004; Hsieh and Huang, 1996; Molina et al., 1999; Safarpour et al., 2004; Sanchez et al., 2003), analysis of minerals in hydrothermal veins (Voicu and Hallbauer, 2005), analysis of trace metals in water and air (Dabek-Zlotorzynska et al., 2003; Fung and Lau, 2001a; Shakulashvili et al., 2000; Yang et al., 2003), oxyanions in groundwater (Fung and Lau, 2001b), analysis of tracers in brine (Kleinmeyer et al., 2001), separation and quantification of Fe species (Rennert and Mansfeldt, 2005; Seidel and Faubel, 1998), Br^- and NO_3 in seawater (Mori et al., 2002), N species (Yao and Xu, 2002), and S species (Chen and Naidu, 2003). Given these advances, the combined use of peepers and CE have applications to a wide range of biogeochemical questions at small scales and can provide insights into linkages between microorganisms, minerals and aqueous solutions. Modifications to field sampling designs could allow resolution of gradients at even finer spatial resolution than presented here.

6. Conclusions

Steep geochemical gradients indicating zones of significant biogeochemical cycling were observed at sediment interfaces within a wetland–aquifer system. Both the sediment–water and silt–sand interfaces appear to be contact zones between waters of different redox potential. At the sediment–water interface, the more oxidizing surface water is a source of electron acceptors to the anoxic wetland sediments while the wetland sediments supply organic acids to serve as electron donors. Similarly, the interface between the upper silt zone and less reducing coarse sand lens marks the contact between zones of differing redox potential. In these unique zones microbial metabolism is enhanced because it benefits from the mixing of electron donors and electron acceptors. Centimeter-scale sampling allowed for resolution of steep geochemical gradients (SO_4^{2-}, Fe, sulfide, NH_4^+, acetate, propionate and butyrate) supporting the idea that increased microbial activity occurs over small spatial scales at mixing interfaces. This resolution was made possible by the use of capillary electrophoresis (CE) to analyze the majority of geochemical parameters on the low sample volumes available in cm-scale porewaters. Data provided in this paper indicates that CE is a powerful tool to quantify geochemical indicators in complex natural waters when sample volumes are limited and suggest that the combination of custom peepers and CE could be used to evaluate geochemical gradients at even finer spatial resolution.

At the sediment–water interface the dominant TEAPs, SO_4^{2-} and Fe reduction, were enhanced by the senescence of an aquatic grass cover. Both processes appear to be occurring at the same location or in reversed thermodynamic order (i.e., SO_4^{2-}

reduction above Fe reduction). These trends can be explained by the abundant electron donors present at the sediment–water interface and by the possible limited availability of reactive Fe compared to the availability of SO_4^{2-}. Below 18 cm, a change in the organic C distribution is evidenced by a sharp increase in the concentration of organic acids, loss of viable seeds, and enhanced SO_4^{2-} reduction (likely of both free SO_4^{2-} and barite). At ~30 cm, SO_4^{2-} decreases to below detection limits allowing organic acids and NH_4^+ to accumulate to high levels reaching 36,000 μM NH_4^+ and 9000 μM acetate. Below this point, these electron donors decrease coincident with the transition to the coarse sand unit. Supersaturated conditions with respect to calcite were observed throughout the profile, and were highest in the water column where more Ca^{2+}, and higher pH were observed likely due to the presence of aquatic vegetation.

This study documents significant cm-scale biogeochemical gradients at various mixing interfaces between a wetland and aquifer contaminated with landfill leachate. These results suggest that quantifying the redox reactions occurring at these relatively small interface zones may be critical to assessing overall biogeochemical cycling in aquifer systems. Inclusion of these active zones in conceptual and numerical models of anaerobic systems would improve understanding of the controls on chemical fate and transport, including the ability of systems to naturally attenuate pollutants. To further quantify the importance of interface processes on system-scale biogeochemical cycling, more detailed knowledge of the spatial and temporal variability of these zones and the rates of various TEAPs should be acquired.

Acknowledgements

We thank Brian Jones, Stephanie McDonald and Erik Smith from Texas A&M University for help with data collection and Dr. Barbara Smallwood for use of equipment and facilities. The research was funded by the National Science Foundation Biocomplexity in the Environment Grant #EAR-0418488, Center of Environmental Rural Health at TAMU Grant #: P30ES09106 and supported by the USGS National Research Program and Toxic Substances Hydrology Program. We thank Scott Christenson, USGS, for field assistance and Jeanne Jaeschke, USGS, for organic acids data verification and two anonymous reviewers for their thoughtful suggestions.[1]

References

Achtnich, C., Bak, F., Conrad, R., 1995. Competition for electron donors among nitrate reducers, ferric iron reducers, sulfate reducers, and methanogens in anoxic paddy soil. Biol. Fert. Soils 19, 65–72.

Adler, M., Hensen, C., Kasten, S., Schulz, H.D., 2000. Computer simulation of deep sulfate reduction in sediments of the Amazon Fan. Int. J. Earth Sci. 88, 641–654.

Albrechtsen, H.-J., Christensen, T.H., 1994. Evidence for microbial iron reduction in a landfill leachate-polluted aquifer (Vejen, Denmark). Appl. Environ. Microbiol. 60, 3920–3925.

APHA, 1975. Standard methods for the examination of water and wastewater, 14th ed. American Public Health Association, Washington, DC.

Aulenta, F., Gossett, J.M., Papini, M.P., Rossetti, S., Majone, M., 2005. Comparative study of methanol, butyrate, and hydrogen as electron donors for long-term dechlorination of tetrachloroethene in mixed anaerobic cultures. Biotechnol. Bioeng. 91, 743–753.

AWWA, APHA, WPCF, 1971. Standard methods for the examination of water and wastewater. American Water Works Association, American Public Health Association, and Water Pollution Control Federation, New York.

Azcue, J.M., Rosa, F., Lawson, G., 1996. An improved dialysis sampler for the in situ collection of larger volumes of sediment pore waters. Environ. Technol. 17, 95–100.

Baedecker, M.J., Cozzarelli, I.M., 1992. The determination and fate of unstable constituents in contaminated ground water. In: Lesage, S., Jackson, R. (Eds.), Groundwater Quality and Analysis at Hazardous Waste Sites. Marcel Dekker, Inc., New York, pp. 425–461.

Baedecker, M.J., Cozzarelli, I.M., Eganhouse, R.P., Siegel, D.E., Bennett, P.C., 1993. Crude oil in a shallow sand and gravel aquifer: 3. Biogeochemical reactions and mass balance modeling in anoxic groundwater. Appl. Geochem. 8, 569–586.

Bally, G., Mesnage, V., Deloffre, J., Clarisse, O., Lafite, R., Dupont, J.P., 2004. Chemical characterization of porewaters in an intertidal mudflat of the Seine estuary: relationship to erosion–deposition cycles. Mar. Pollut. Bull. 49, 163–173.

Baun, A., Reitzel, L.A., Ledin, A., Christensen, T.H., Bjerg, P.L., 2003. Natural attenuation of xenobiotic organic compounds in a landfill leachate plume (Vejen, Denmark). J. Contam. Hydrol. 65, 269–291.

Bekins, B.A., Cozzarelli, I.M., Godsy, E.M., Warren, E., Essaid, H.I., Tuccillo, M.E., 2001. Progression of natural attenuation processes at a crude oil spill site: II. Controls on spatial distribution of microbial populations. J. Contam. Hydrol. 53, 387–406.

Blodau, C., Hoffmann, S., Peine, A., Peiffer, S., 1998. Iron and sulfate reduction in the sediments of acidic mine lake 116 (Brandenburg, Germany). Water Air Soil Pollut. 108, 249–270.

[1] Use of tradenames is for identification purposes only and does not constitute endorsement by the US Geological Survey.

Boschker, H.T.S., Nold, S.C., Wellsbury, P., Bos, D., de Graaf, W., Pel, R., Parkes, R.J., Cappenberg, T.E., 1998. Direct linking of microbial populations to specific biogeochemical processes by C-13-labelling of biomarkers. Nature 392, 801–805.

Breit, G.N., Tuttle, M.L.W., Cozzarelli, I.M., Christenson, S.C., Jaeschke, J.B., Fey, D.L., Berry, C.J., 2005. Results of chemical and isotopic analyses of sediment and water from alluvium of the Canadian River near a closed municipal landfill, Norman, Oklahoma. US Department of Interior and US Geol. Surv.: Toxic Hydrology Program, Open-File Rep. 2005-1091, pp. 1–37.

Capone, D.G., Kiene, R.P., 1988. Comparison of microbial dynamics in marine and freshwater sediments: Contrasts in anaerobic carbon catabolism. Limnol. Oceanogr. 33, 725–749.

Champ, D.R., Gulens, J., Jackson, R.E., 1979. Oxidation–reduction sequences in groundwater flow systems. Can. J. Earth Sci. 127, 85–108.

Chapelle, F.H., Mcmahon, P.B., 1991. Geochemistry of dissolved inorganic carbon in a coastal-plain aquifer: 1. Sulfate from confining beds as an oxidant in microbial CO_2 production. J. Hydrol. 127, 85–108.

Chapelle, F.H., Haack, S.K., Adriaens, P., Henry, M., Bradley, P.M., 1996. Comparison of Eh and H_2 measurements for delineating redox processes in a contaminated aquifer. Environ. Sci. Technol. 30, 3565–3569.

Chen, Z.L., Naidu, R., 2003. Separation of sulfur species in water by co-electroosmotic capillary electrophoresis with direct and indirect UV detection. Int. J. Environ. Anal. Chem. 83, 749–759.

Christensen, T.H., Bjerg, P.L., Banwart, S., Jakobsen, R., Heron, G., Albrechtsen, H.J., 2000. Characterization of redox conditions in groundwater contaminant plumes. J. Contam. Hydrol. 45, 165–241.

Ciglenecki, I., Caric, M., Krsinic, F., Vilicic, D., Cosovic, B., 2005. The extinction by sulfide-turnover and recovery of a naturally eutrophic, meromictic seawater lake. J. Mar. Syst. 56, 29–44.

Cozzarelli, I.M., Baedecker, M.J., Eganhouse, R.P., Goerlitz, D.F., 1994. The geochemical evolution of low-molecular-weight organic acids derived from the degradation of petroleum contaminants in groundwater. Geochim. Cosmochim. Acta 58, 863–877.

Cozzarelli, I.M., Herman, J.S., Baedecker, M.J., Fischer, J.M., 1999a. Geochemical heterogeneity of a gasoline-contaminated aquifer. J. Contam. Hydrol. 40, 261–284.

Cozzarelli, I.M., Suflita, J.M., Ulrich, G.A., Harris, S.H., Scholl, M.A., Schlottmann, J.L., Jaeschke, J.B., 1999b. Biogeochemical processes in a contaminant plume downgradient from a landfill, Norman, Oklahoma. Investigations Report 99-4018C Subsurface Contamination from Point Sources: US Geol. Survey Water-Resour. 3, pp. 521–530.

Cozzarelli, I.M., Suflita, J.M., Ulrich, G.A., Harris, S.H., Schroll, M.A., Schlottmann, J.L., Christenson, S., 2000. Geochemical and microbiological methods for evaluating anaerobic processes in an aquifer contaminated by landfill leachate. Environ. Sci. Technol. 34, 4025–4033.

Cozzarelli, I.M., Bekins, B.A., Baedecker, M.J., Aiken, G.M., Eganhouse, R.P., Tuccillo, M.E., 2001. Progression of natural attenuation processes at a crude-oil spill site: I. Geochemical evolution of the plume. J. Contam. Hydrol. 53, 369–385.

Dabek-Zlotorzynska, E., Kelly, M., Chen, H., Chakrabarti, C.L., 2003. Evaluation of capillary electrophoresis combined with a BCR sequential extraction for determining distribution of Fe, Zn, Cu, Mn, and Cd in airborne particulate matter. Anal. Chim. Acta 498, 175–187.

Dabek-Zlotorzynska, E., Aranda-Rodriguez, R., Graham, L., 2005. Capillary electrophoresis determinative and GC–MS confirmatory method for water-soluble organic acids in airborne particulate matter and vehicle emission. J. Sep. Sci. 28, 1520–1528.

Dahm, C.N., Grimm, N.B., Marmonier, P., Valett, H.M., Vervier, P., 1998. Nutrient dynamics at the interface between surface waters and groundwaters. Freshwater Biol. 40, 427–451.

Devlin, J.F., 1991. Field evidence for the effect of acetate on leachate alkalinity. Ground Water 28, 863–867.

Duddleston, K.N., Kinney, M.A., Kiene, R.P., Hines, M.E., 2002. Anaerobic microbial biogeochemistry in a northern bog: acetate as a dominant metabolic end product. Global Biogeochem. Cycles 16, 11-1–11-9.

Eganhouse, R.P., Cozzarelli, I.M., Scholl, M.A., Matthews, L.L., 2001. Natural attenuation of volatile organic compounds (VOCs) in the leachate plume of a municipal landfill: using alkylbenzenes as process probes. Ground Water 39, 192–202.

Frías, S., Sánchez, M.J., Rodríguez, M.A., 2004. Determination of triazine compounds in ground water samples by micellar electrokinetic capillary chromatography. Anal. Chim. Acta 503, 271–278.

Fung, Y.F., Lau, K.M., 2001a. Determination of trace metals by capillary electrophoresis. Electrophoresis 22, 2192–2200.

Fung, Y.S., Lau, K.M., 2001b. Determination of oxoanions in river water by capillary electrophoresis. Electrophoresis 22, 2251–2259.

Grossman, E.L., Cifuentes, L.A., Cozzarelli, I.M., 2002. Anaerobic methane oxidation in a landfill-leachate plume. Environ. Sci. Technol. 36, 2436–2442.

Hemond, H.F., 1990. Acid neutralizing capacity, alkalinity, and acid–base status of natural waters containing organic acids. Environ. Sci. Technol. 24, 1486–1489.

Hesslein, R.H., 1976. An in situ sampler for close interval pore water studies. Limnol. Oceanogr. 21, 912–914.

Hines, M.E., Knollmeyer, S.L., Tugel, J.B., 1989. Sulfate reduction and other sedimentary biogeochemistry in a northern New England salt marsh. Limnol. Oceanogr. 34, 578–590.

Hines, M.E., Banta, G.T., Giblin, A.E., Hobbie, J.E., Tugel, J.B., 1994. Acetate concentrations and oxidation in salt-marsh sediments. Limnol. Oceanogr. 39, 140–148.

Ho, T.Y., Scranton, M.I., Taylor, G.T., Varela, R., Thunell, R.C., Muller-Karger, F., 2002. Acetate cycling in the water column of the Cariaco Basin: seasonal and vertical variability and implication for carbon cycling. Limnol. Oceanogr. 47, 1119–1128.

Hsieh, Y.Z., Huang, H.Y., 1996. Analysis of chlorophenoxy acid herbicides by cyclodextrin-modified capillary electrophoresis. J. Chromatogr. A 745, 217–223.

Huang, X.F., Hu, M., He, L.Y., Tang, X.Y., 2005. Chemical characterization of water-soluble organic acids in PM2.5 in Beijing, China. Atmos. Environ. 39, 2819–2827.

Hunt, R.J., Krabbenhoft, D.P., Anderson, M.P., 1997. Assessing hydrogeochemical heterogeneity in natural and constructed wetlands. Biogeochemistry 39, 271–293.

Jacobs, P.H., 2002. A new rechargeable dialysis pore water sampler for monitoring sub-aqueous in-situ sediment caps. Water Res. 36, 3121–3129.

Jones, W.B., Cifuentes, L.A., Kaldy, J.E., 2003. Stable carbon isotope evidence for coupling between sedimentary bacteria and seagrasses in a sub-tropical lagoon. Mar. Ecol. Prog. Ser. 255, 15–25.

Kantrud, H.A. 1990. Sago pondweed (Potamogeton pectinatus L.): a literature review [Online]. Available by US Fish and Wildlife Service, Fish and Wildlife Resource Publication 176. (posted Version 16JUL97; verified April 29, 2006).

Kappler, A., Emerson, D., Edwards, K., Amend, J.P., Gralnick, J.A., Grathwohl, P., Hoehler, T., Straub, K.L., 2005. Microbial activity in biogeochemical gradients-new aspects of research. Geobiology 3, 229–233.

Kharaka, Y.K., Ambats, G., Thordsen, J.J., 1993. Distribution and significance of dicarboxylic-acid anions in oil-field waters. Chem. Geol. 107, 499–501.

Kleikemper, J., Schroth, M.H., Sigler, W.V., Schmucki, M., Bernasconi, S.M., Zeyer, J., 2002. Activity and diversity of sulfate-reducing bacteria in a petroleum hydrocarbon-contaminated aquifer. Appl. Environ. Microbiol. 68, 1516–1523.

Kleinmeyer, J.A., Rose, P.E., Harris, J.M., 2001. Determination of ultratrace-level fluorescent tracer concentrations in environmental samples using a combination of HPLC separation and laser-excited fluorescence multiwavelength emission detection: application to testing of geothermal well brines. Appl. Spectros. 55, 690–700.

Koch, M.S., Mendelssohn, I.A., Mckee, K.L., 1990. Mechanism for the hydrogen sulfide-induced growth limitation in wetland macrophytes. Limnol. Oceanogr. 35, 399–408.

Koretsky, C.M., Moore, C.M., Lowe, K.L., Meile, C., Dichristina, T.J., Van Cappellen, P., 2003. Seasonal oscillation of microbial iron and sulfate reduction in saltmarsh sediments (Sapelo Island, GA, USA). Biogeochemistry 64, 179–203.

Koretsky, C.M., Van Cappellen, P., DiChristina, T.J., Kostka, J.E., Lowe, K.L., Moore, C.M., Roychoudhury, A.N., Viollier, E., 2005. Salt marsh pore water geochemistry does not correlate with microbial community structure. Estuar. Coast. Shelf Sci. 62, 233–251.

Kostka, J.E., Roychoudhury, A., Van Cappellen, P., 2002. Rates and controls of anaerobic microbial respiration across spatial and temporal gradients in saltmarsh sediments. Biogeochemistry 60, 49–76.

Linhardt, R.J., Toida, T., 2002. Ultra-high resolution separation comes of age (capillary electrophoresis). Science 298, 1441–1442.

Llobet-Brossa, E., Rabus, R., Bottcher, M.E., Konneke, M., Finke, N., Schramm, A., Meyer, R.L., Grotzschel, S., Rossello-Mora, R., Amann, R., 2002. Community structure and activity of sulfate-reducing bacteria in an intertidal surface sediment: a multi-method approach. Aquat. Microb. Ecol. 29, 211–226.

Lorah, M.M., Cozzarelli, I.M., Böhlke, J.K., submitted for publication. Biogeochemical effect of interaction of a landfill leachate plume with a seasonally ponded wetland (slough). J. Contam. Hydrol.

Lovley, D.R., Phillips, E.J.P., 1987. Competitive mechanisms for the inhibition of sulfate reduction and methane production in the zone of ferric iron reduction in sediments. Appl. Environ. Microbiol. 53, 2636–2641.

Lovley, D.R., Phillips, E.J.P., Lonergan, D.J., 1991. Enzymatic versus nonenzymatic mechanisms for Fe(III) reduction in aquatic sediments. Environ. Sci. Technol. 25, 1062–1067.

Ludvigsen, L., Albrechtsen, H.-J., Heron, G., Bjerg, P.L., Christensen, T.H., 1998. Anaerobic microbial processes in a landfill leachate contaminated aquifer (Grindsted, Denmark). J. Contam. Hydrol. 33, 273–291.

Lyngkilde, J., Christensen, T.H., 1992. Fate of organic contaminants in the redox zones of a landfill leachate pollution plume (Vejen, Denmark). J. Contam. Hydrol. 10, 291–307.

Mayer, K.U., Benner, S.G., Frind, E.O., Thornton, S.F., Lerner, D.N., 2001. Reactive transport modeling of processes controlling the distribution and natural attenuation of phenolic compounds in a deep sandstone aquifer. J. Contam. Hydrol. 53, 341–368.

McGuire, J.T., Smith, E.W., Long, D.T., Hyndman, D.W., Haack, S.K., Klug, M.J., Velbel, M.A., 2000. Temporal variations in parameters reflecting terminal-electron-accepting processes in an aquifer contaminated with waste fuel and chlorinated solvents. Chem. Geol. 169, 471–485.

McGuire, J.T., Long, D.T., Klug, M.J., Haack, S.K., Hyndman, D.W., 2002. Evaluating behavior of oxygen, nitrate, and sulfate during recharge and quantifying reduction rates in a contaminated aquifer. Environ. Sci. Technol. 36, 2693–2700.

McMahon, P.B., 2001. Aquifer/aquitard interfaces: mixing zones that enhance biogeochemical reactions. Hydrogeol. J. 9, 34–43.

McMahon, P.B., Chapelle, F.H., 1991. Microbial-production of organic-acids in aquitard sediments and its role in aquifer geochemistry. Nature 349, 233–235.

Molina, M., Perez-Bendito, D., Silva, M., 1999. Multi-residue analysis of *N*-methylcarbamate pesticides and their hydrolytic metabolites in environmental waters by use of solid-phase extraction and micellar electrokinetic chromatography. Electrophoresis 20, 3439–3449.

Mori, M., Hu, W., Haddad, P.R., Fritz, J.S., Tanaka, K., Tsue, H., Tanaka, S., 2002. Capillary electrophoresis using high ionic strength background electrolytes containing zwitterionic and non-ionic surfactants and its application to direct determination of bromide and nitrate in seawater. Anal. Bioanal. Chem. 372, 181–186.

Motelica-Heino, M., Naylor, C., Zhang, H., Davison, W., 2003. Simultaneous release of metals and sulfide in lacustrine sediment. Environ. Sci. Technol. 37, 4374–4381.

Nealson, K.H., 1997. Sediment bacteria: who's there, what are they doing, and what's new?. Ann. Rev. Earth Planet. Sci. 25 403–434.

Nicholson, R.V., Cherry, J.A., Reardon, E.J., 1983. Migration of contaminants in groundwater at a landfill: a case study. J. Hydrol. 63, 131–176.

Parkhurst, D.L., 1995. PHREEQC: User's guide to PHREEQC: a computer program for speciation, reaction-path, advective-transport, and inverse geochemical calculations. US Geol. Surv. Water Resour., Investig. Rep. 95-4227, pp. 1–143.

Peterson, J.N., Sun, Y., 2000. An analytical solution evaluating steady-state plumes of sequentially reactive contaminants. Transport Porous Med. 41, 287–303.

Postma, D., Jakobsen, R., 1996. Redox zonation: equilibrium constraints on the Fe(III)/SO_4-reduction interface. Geochim. Cosmochim. Acta 60, 3169–3175.

Rennert, T., Mansfeldt, T., 2005. Iron-cyanide complexes in soil under varying redox conditions: speciation, solubility and modelling. Eur. J. Soil Sci. 56, 527–536.

Reynolds Jr., R.C., 1978. Polyphenol inhibition of calcite precipitation in Lake Powell. Limnol. Oceanogr. 23, 585–597.

Röling, W.F.M., van Breukelen, B.M., Braster, M., Lin, B., van Verseveld, H.W., 2001. Relationships between microbial community structure and hydrochemistry in a landfill leachate-polluted aquifer. Appl. Environ. Microbiol. 67, 4619–4629.

Safarpour, H., Asiaie, R., Katz, S., 2004. Quantitative analysis of imazamox herbicide in environmental water samples by capillary electrophoresis electrospray ionization mass spectrometry. J. Chromatogr. A 1036, 217–222.

Sanchez, M.E., Rabanal, B., Otero, M., Martin-Villacorta, J., 2003. Solid-phase extraction for the determination of dimethoate in environmental water and soil samples by micellar electrokinetic capillary chromatography (MEKC). J. Liquid Chromatogr. Relat. Technol. 26, 545–557.

Sass, A.M., Eschemann, A., Kuhl, M., Thar, R., Sass, H., Cypionka, H., 2002. Growth and chemosensory behavior of sulfate-reducing bacteria in oxygen-sulfide gradients. FEMS Microbiol. Ecol. 40, 47–54.

Schlesinger, W.H., 1997. Biogeochemistry: An Analysis of Global Change, second ed. Academic Press, San Diego, CA.

Scholl, M.A., Christenson, S., 1998. Spatial variation in hydraulic conductivity determined by slug tests in the Canadian River alluvium near the Norman Landfill, Norman, Oklahoma. US Geol. Surv. Water-Resour. Investig. Rep. 97-4292.

Scholl, M.A., Christenson, S.C., Cozzarelli, I.M., 2005. Recharge processes in an alluvial aquifer riparian zone, Norman Landfill, Norman, Oklahoma, 1998–2000. US Geol. Surv. Sci. Investig. Rep. 2004-5238, pp. 1–60.

Seidel, B.S., Faubel, W., 1998. Determination of iron in real samples by high performance capillary electrophoresis in combination with thermal lensing. Fresen. J. Anal. Chem. 360, 795–797.

Sène, M., Doré, T., Pellissier, F., 2000. Effect of phenolic acids in soil under and between rows of a prior sorghum (*Sorghum bicolor*) crop on germination, emergence, and seedling growth of peanut (*Arachis hypogea*). J. Chem. Ecol. 26, 625–637.

Shakulashvili, N., Faller, T., Engelhardt, H., 2000. Simultaneous determination of alkali, alkaline earth and transition metal ions by capillary electrophoresis with indirect UV detection. J. Chromatogr. A 895, 205–212.

Shannon, R.D., White, J.R., 1996. The effects of spatial and temporal variations in acetate and sulfate on methane cycling in two Michigan peatlands. Limnol. Oceanogr. 41, 435–443.

Stacy, B.L., 1961. Ground water resources of the alluvial deposits of the Canadian River valley near Norman, Oklahoma. US Geol. Surv. Open-File Rep. 61-177.

Tuxen, N., Albrechtsen, H.-J., Bjerg, P.L., 2006. Identification of a reactive degradation zone at a landfill leachate plume fringe using high resolution sampling and incubation techniques. J. Contam. Hydrol. 85, 179–194.

Ulrich, G.A., Martino, D., Burger, K., Routh, J., Grossman, E.L., Ammerman, J.W., Suflita, J.M., 1998. Sulfur cycling in the terrestrial subsurface: commensal interactions, spatial scales, and microbial heterogeneity. Microbial Ecol. 36, 141–151.

Ulrich, G.A., Breit, G., Cozzarelli, I.M., 2003. Sources of sulfate supporting anaerobic metabolism in a contaminated aquifer. Environ. Sci. Technol. 37, 1093–1099.

van Breukelen, B.M., Griffioen, J., 2004. Biogeochemical processes at the fringe of a landfill leachate plume: potential for dissolved organic carbon, Fe(II), Mn(II), NH_4, and CH_4 oxidation. J. Contam. Hydrol. 73, 181–205.

van Breukelen, B.M., Röling, W.F.M., Groen, J., Griffioen, J., van Verseveld, H.W., 2003. Biogeochemistry and isotope geochemistry of a landfill leachate plume. J. Contam. Hydrol. 65, 245–268.

van Breukelen, B.M., Griffioen, J., Röling, W.F.M., van Verseveld, H.W., 2004. Reactive transport modelling of biogeochemical processes and carbon isotope geochemistry inside a landfill leachate plume. J. Contam. Hydrol. 70, 249–269.

Voicu, G., Hallbauer, D.K., 2005. Determination of the physicochemical characteristics of hydrothermal fluids from the post-metamorphic Omai gold deposit, Guiana Shield, using analysis of ionic species by crush-leach technique and capillary electrophoresis. Miner. Petrol. 83, 243–270.

Webster, I.T., Teasdale, P.R., Grigg, N.J., 1998. Theoretical and experimental analysis of peeper equilibration dynamics. Environ. Sci. Technol. 32, 1727–1733.

Wellsbury, P., Parkes, R.J., 1995. Acetate bioavailability and turnover in an estuarine sediment. FEMS Microbiol. Ecol. 17, 85–94.

Wu, C.H., Lo, Y.S., Nian, H.C., Lin, Y.Y., 2003. Capillary electrophoretic analysis of the derivatives and isomers of benzoate and phthalate. J. Chromatogr. A 1003, 179–187.

Yang, W.P., Zhang, Z.J., Deng, W., 2003. Simultaneous, sensitive and selective on-line chemiluminescence determination of Cr(III) and Cr(VI) by capillary electrophoresis. Anal. Chim. Acta 485, 169–177.

Yao, W., Xu, S.K., 2002. Determination of nitrate and nitrite in environmental water samples with direct ultraviolet detection by flow injection-capillary electrophoresis. Chin. J. Anal. Chem. 30, 836–838.